DEVELOPING AND PRACTICING OF QUASI-Z-SOURCE ELECTRIC VEHICLE BATTERY CHARGER.

Gaurangi A. Sawant[1], Tanvi Santosh Maske[2], Sayujyata Mahesh Khot[3], Kiran Namdev Jagtap[4] , Nitin B. Sawant[5] , Kalpesh S. Kamble[6] ,
[1,2,3,4] (Department of Electrical Engineering, SSPM's COE, A/P-Harkul Budruk, Tal- Kankavli. Dist-Sindhudurg, India,
[5] (Department of Electrical Engineering, SSPM's COE, A/P-Harkul Budruk, Tal-Kankavli. Dist-Sindhudurg, India,
[6] (Department of Mechanical Engineering, SSPM's COE, A/P-Harkul Budruk, Tal-Kankavli. Dist-Sindhudurg, India,

ABSTRACT: The quasi Z-source fed phase shift full bridge converter is part of the suggested charger. In this two-stage dc-dc conversion, a phase shift full bridge converter lowers the high DC voltage needed to charge the battery efficiently while the quasi Z-source is used for power factor correction and harmonic distortion reduction. Using MATLAB simulation, the charger's performance is examined. The proposed charger demonstrated at 90% charger efficiency, a power factor of unity, and a low harmonic distortion of 3.53% in the experimental results.
The primary energy source of an electric vehicle is a sizable rechargeable battery pack. Battery chargers that use traditional iron core transformers are large and ineffective. Chargers for electric vehicles need to be powerful, lightweight, and have a high power density. This research paper emphasises studies and designs a lithium ion battery electric car charger that can be used with light-duty electric automobiles.

Keywords: DC to DC converter, electric car, battery charger, power factor, harmonics and quasi-Z-source converter.

I. INTRODUCTION:

Electric two- and three-wheelers are now commonly employed in cities for both private and public transportation. Along with their many benefits—such as great energy efficiency, low maintenance costs, zero emissions, and cheap operating costs—electric vehicles (EVs) nevertheless face a number of obstacles to widespread adoption, including limited charging infrastructure, long battery charging times, and limited driving range. The demand for both portable home chargers and charging stations has surged due to the significant increase in the use of electric two- and three-wheelers. It is therefore essential to provide quick, portable, and effective chargers that may shorten battery charging times and preserve the integrity of batteries [1].

The current focus of battery charger design research is on quick charging, yet the device still needs to be lightweight, efficient, and achieve unity power factor. For battery chargers, [2] suggests using a Phase Shift Full Bridge (PSFB) converter in conjunction with a traditional diode rectifier. Nevertheless, the power factor and supply harmonics are adversely affected when diode rectifiers are used. Furthermore, power electronics-based battery chargers with high frequency ferrite core transformers show more than 90% efficiency and also weigh less than conventional chargers that employ iron-core transformers, which have an efficiency of less than 80% [3].

Quasi Z-Source (QZS) converters address the drawbacks of traditional voltage or current source converters that operate in either boost or buck mode [7]. All of the benefits of a standard Z-source converter are included in a QZS converter, including immunity to EMI noise, suitability for a variety of converter applications (DC-DC, DC-AC, and AC-AC), and the ability to buck and boost. With a lower duty cycle and less instability brought on by inductor saturation, the QZS converter achieves a high boost factor [4-5, 8]. Furthermore, the QZS converter offers the benefit of a shared grounding line connecting the input and output [9].

In addition, compared to a conventional Z-source converter, it lessens the voltage stress on the impedance network capacitor. Owing to these benefits, the suggested charger uses a QZS converter to address the power factor and harmonic distortion of the AC supply. It simultaneously keeps the DC output current and voltage constant. Additionally, the PSFB converter's adoption boosts the capacity to handle voltage and power [11]. Zero voltage switching lowers electromagnetic interference and increases charger efficiency when using the shoot through mode of a QZS fed PSFB dc-dc converter [6, 12–14].

The paper is divided into several sections. In section II, the suggested charging mechanism and how it operates are described. In section III, analysis and circuit design are covered.In section IV, the simulation findings used to illustrate charger performance are explained. Section V of the study discusses the conclusion.

II. PROPOSED CHARGER SYSTEM:

DC voltage is produced from AC input using a diode rectifier. The QZS converter is then given the diode rectifier's DC output voltage. In order to supply the appropriate DC voltage level needed as input for a MOSFET-based PSFB converter, the QZS converter functions as a boost converter. The conventional voltage and current source converters, which can work in boost or buck mode, have theoretical and conceptual restrictions. By placing a QZS converter behind a diode rectifier, the problems with traditional voltage source converters are resolved. As illustrated in Figure 1, the QZS network is composed of a filter circuit with two diodes (D1), two capacitors (C1, C2), and two inductors (L1, L2).

Following the QZS network, a MOSFET, diode, and filter capacitor are connected to regulate the output voltage and reduce output voltage and current ripples. At an extremely high PWM switching frequency, the MOSFET is used.

The converter's shoot-through duty ratio can be adjusted to manage the output voltage. MOSFET is turned ON during the shoot-through state, which results in a short circuit throughout the QZS network. [02]

As was previously said, the QZS converter can only increase the output voltage. After the QZS converter, an extra converter is required to accomplish the buck mode of operation. Thus, the suggested battery charger design incorporates the PSFB architecture. As illustrated in Figure 1, it is composed of a high frequency full bridge inverter, a full bridge rectifier, a transformer, and an output filter circuit. This design is known as an isolated DC/DC converter since it uses a high frequency transformer. Galvanic isolation between the grid supply and the battery, which is necessary in all battery charger circuits, is provided by the use of transformers. The weight and dimensions of the charger are decreased using a high frequency ferrite core transformer, which also aids in maintaining high charger DC voltage is initially converted to high frequency AC voltage via a PSFB converter. Prior to being converted to the appropriate DC voltage needed to charge the lithium ion battery, the PSFB converter first transforms DC voltage to high frequency AC voltage. [06]

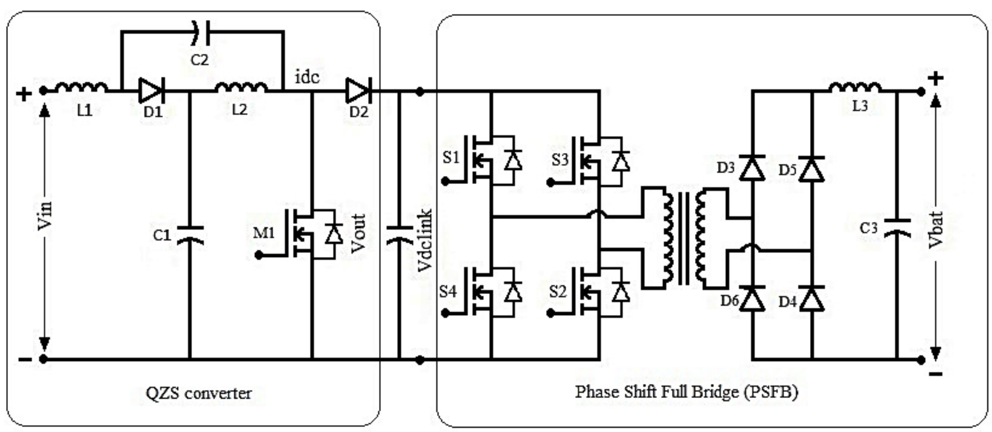

Fig. 1. Circuit diagram of proposed charger system.

III. THE CHARGER SYSTEM'S ANALYSIS:

A. QZS converter:

Mode 1 and Mode 2 are the two operating modes. Shoot-through is referred to as mode 1, and non-shoot-through is referred to as mode 2.

Mode 1: To access this mode, turn on the QZS converter's power MOSFET. As can be seen in Figure 2, the diode D1 operates in the forward biassed mode when the output voltage Vout of the QZS converter is less than the applied voltage Vin. Consequently, the QZS converter operates in the energy-storing mode when in this state. The QZS network's filter components gather and store energy from input. The shoot-through duty ratio and switching frequency are calibrated to prevent inductors from becoming saturated. [07]

EQUATION:

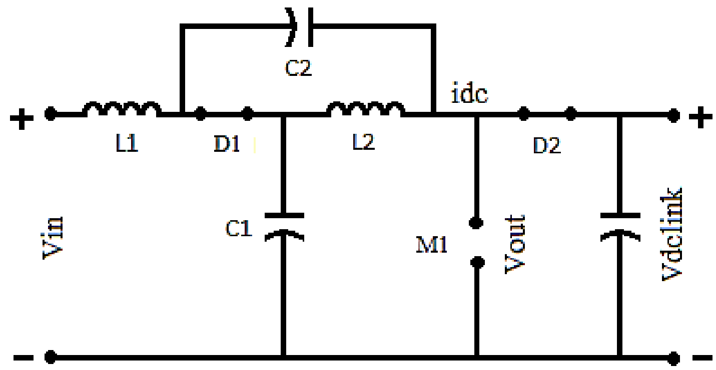

Fig. 2. Mode 1 (non shoot-through) operation.

Where v1, v2, and vi are the voltages across capacitors C1, C2, and input voltage, respectively, and i, j, and k are the currents flowing through inductor L1, L2, and dc link, respectively.

Mode 2: In this non-shoot-through mode, the diode D1 operates in blocking mode, as seen in Figure 3, when the QZS output voltage V_{out} is greater than the applied voltage V_{in}. Consequently, the QZS converter displays boost operation mode in this state.

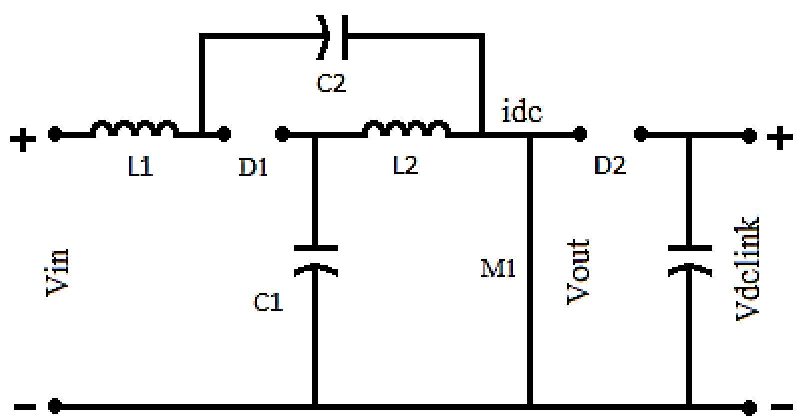

Fig. 3. Mode 2 (shoot-through) operations.

Duty cycle D of a switching device is written as;

$D = \mathrm{T0}/$

$(\mathrm{T0} + T0FF)$

On the other hand, mode 2 time is recorded as T_{ON}, and mode 1 time is recorded as T_{OFF}. Using the formulas for current, voltage, and duty cycle mentioned above, the capacitor voltage V_{C1} is found by,

$$VC1 = \frac{(1-D)}{D} * VC2$$

Consequently, the relationship between the QZS converter's output voltage (Vout) and input voltage (Vin) is established by utilising,

$V_{out} = V_{C1} + V_{C2}$.

The output voltage should theoretically tend to infinity at 0.5 duty cycle. Thus, a duty cycle of less than 0.5 is recommended for the QZS converter. [08]

B. PSFB converter design:

The PSFB dc-dc converter architecture is used in the suggested charger. Full bridge diode rectifier on secondary side of transformer and full bridge inverter on primary side make up PSFB converter. These switches operate with a 400V supply and a 20A current. A 50kHz phase-shifted PWM signal operates the four switches of a complete bridge inverter. In order to charge a 48V lithium ion battery, it is utilised for dc-dc conversion, which transforms a high dc voltage in the 400V region into a low voltage. Additionally, it provides zero voltage switching, which lowers switching losses and raises converter efficiency. For the following parameters, PSFB topology is used in the construction of the 2kW charger. [10]

PSFB input voltage,

$Vdclink$ = 400V

PSFB output voltage,

$Vbat$ = 55V

Output current, Io = 20A

Switching frequency fs = 50 kHz

1) Ferrite core transformer design:

The purpose of the PSFB with high frequency ferrite core transformer is to reduce the system voltage from 400V to 55V. A transformer core of 1 cm2 in cross-section area and having a maximum flux density of 0.2 T, or 2000 G, is chosen. Np is calculated for Keff as 0.36, the major side number of turns, from

$$Np = \frac{Vdclink \times Keff \times 10^8}{2 \times Bmax \times A \times fs}$$

72 turns make up the primary turns Np. The secondary side number of turns, Ns, is then calculated using the PSFB converter duty cycle of K and the transformation ratio T. For a given transformation ratio T, the maximum duty cycle K is expressed as 0.4.,

$$K = \frac{Vbat}{Vsec}$$

Consequently, in order to get the intended Vbat of 55V, the secondary side voltage Vsec needs to be 137.5V. Using equation 13, this means that the secondary side number of turns Ns is approximately 24 turns.[15]

2) Filter inductor design:

The voltage across output filter inductor VLO is given by

$$V_L = (5V_{dclink} - V_{bat})$$

For efficiency η of 0.9, the VLwill be 305V.

$$L = \frac{V_L \times K_{eff}}{\Delta I_L \times f_s}$$

$$L = 1.098\ mH$$

where the effective duty cycle (Keff) is 0.36 and the switching frequency (fs) is 50kHz. Using equation 16, the filter inductor value for 10% of the inductor current ripple, ΔIL, is 1.098mH.

3) Output capacitor design:

With the, Switching frequency of 50 kHz, output voltage ripple ΔV_{bat} as 0.5V and the output capacitor C is obtained from the equation;

$$\Delta Vbat = [Vbat\ (1 - Keff)]\ /\ [16 \times fs2 \times C \times L]$$

For the effective duty cycle Keff = 0.36, the output capacitor is 1.6μf.

IV. RESULT AND DISCUSSION:

The charging mechanism is simulated using Matlab/Simulink software. Figure 4 illustrates the charger circuit that was created and constructed using Simulink software to evaluate its functionality. Evaluations are made of supply power factor, harmonic distortion, converter efficiency, and battery charging performance. The following is a list of the system's input-output parameters:

Input voltage: 230V/50Hz AC

DC link voltage: 400V
Output DC voltage: 50-55V
Battery: 48V/50A
Switching frequency of PFC stage: Hysteresis control
Switching frequency of PSFB converter: 50 kHz

After the diode rectifier, the QZS PFC converter stage is connected. Its functioning is managed by a current hysteresis control method-based variable frequency, variable duty cycle control technique. This control approach generates an error signal by measuring the QZS converter's output DC link voltage (Vdclink) and comparing it to the set-point voltage (400V). After applying the generated error signal to the PI controller, a control signal is produced. This control signal is then multiplied by the absolute value of the input ac voltage to produce the current reference signal. The final control signal is generated and supplied to the hysteresis-based PWM generating block after a comparison between the generated current reference and the actual input ac current. The switch in the QZS PFC converter is then supplied with the output PWM signal. Figure 5 displays the input voltage, current, and DC link voltage. The hysteresis control approach has many benefits. It lowers input current harmonic distortion and boosts power factor by causing the input ac current to fluctuate in phase with the input ac voltage as soon as the circuit is turned on. Three to four supply voltage cycles are needed for the output response to stabilize. [15]

The PFC stage helps to minimise output DC voltage ripples in terms of voltage and current while lowering THD and increasing power factor. The input ac current (Iin) waveform is sinusoidal and in phase with the input voltage (Vin), as seen in fig. 5. The DC/DC converter receives the constant DC voltage (Vdc-link) of 400V from the PFC stage, which regulates the unregulated output voltage of the diode rectifier. The resulting DC connection voltage has minor (<10%) double frequency voltage ripples. The supply current is distorted by a third harmonic, albeit its value is less than 3.5%. [14]

The FFT analysis tool in Simulink is used to calculate the total harmonic distortion (THD), as illustrated in Figure 6. With a THD of 3.53% and a power factor of 0.99—that is, almost one—the AC supply satisfies the IEEE industrial standard IEEE 519-2014. [12]

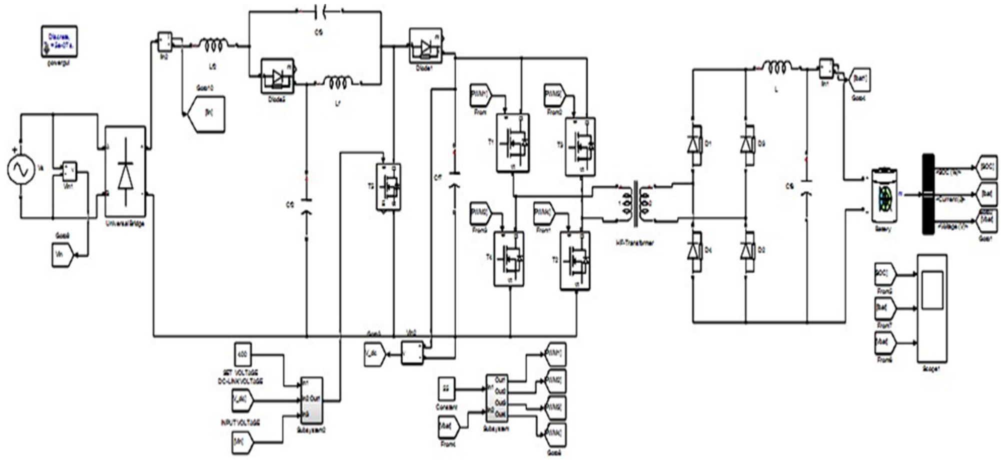

Fig. 4. Simulink diagram of proposed battery charger system.

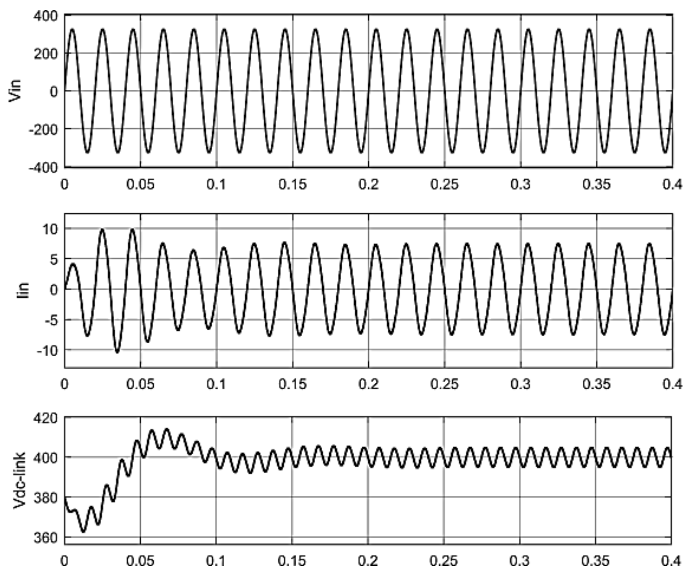

Fig. 5. Input voltage (Vin), current (Iin) and DC link voltage (Vdclink) waveforms.

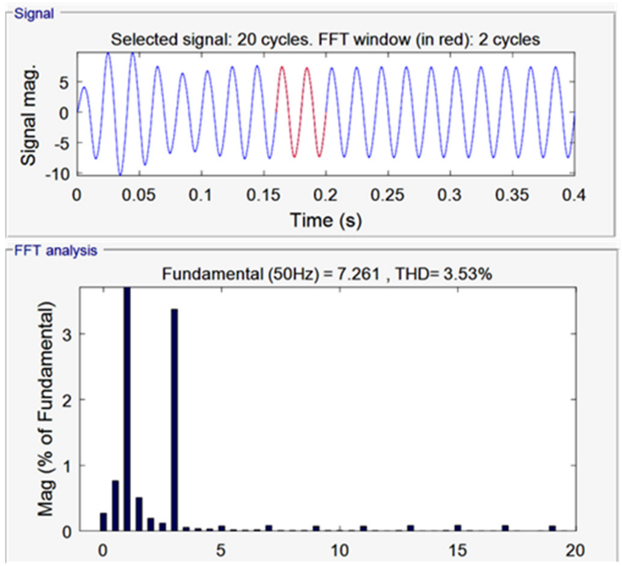

Fig. 6. THD analysis result of input AC current

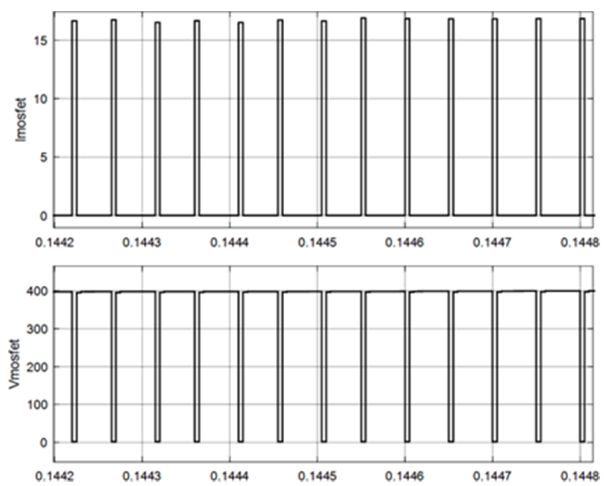

Fig. 7. MOSFET voltage and current waveforms.

In the PFC step, MOSFETs are used as power switching devices. Figure 7 illustrates the maximum MOSFET voltage and current, which are 400V and 18A, respectively. Thus, MOSFETs that are widely available in the market and have voltage and current ratings of 500V and 25A can be utilised in hardware circuits.

In order to charge a battery, a full bridge phase shift converter is utilised as a DC/DC converter. It reduces a high voltage of 400V to a lesser value of 50–55V. The lithium ion battery is charged using a constant current, constant voltage charging method. This control system uses two PI controllers, one of which generates a control signal matching to the battery voltage and the other to the battery current. The phase shift between two PWM signals is controlled by the control signal that is produced when the two PI controllers operate in unison. These 50kHz PWM signals are created and applied to four power switches of a full bridge phase shift converter, together with their complementary output signals.

Figure 8 displays the converter's resulting output voltage spanning the primary, secondary, and battery charging voltages. [15]

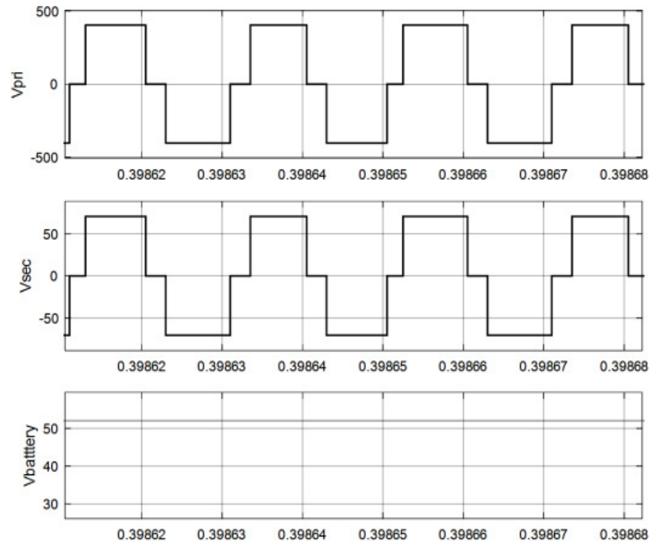

Fig. 8. Isolation transformer primary, secondary and battery charging voltage.

The primary load in the circuit is a 48V/50A lithium ion battery type. As seen in Figure 9, the battery SoC is initially set to 30%. The battery voltage and SoC then steadily increase while the current stays constant. [15]

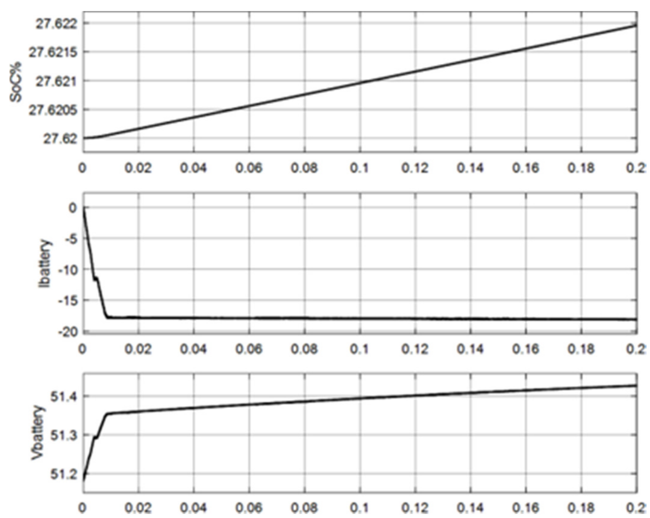

Fig. 9. Battery SoC, current and voltage.

Negative battery current implies that the battery is charging. In steady state battery charging voltage is 52V and current is 19A, so total output power is about 988W. The input power supplied to the circuit is about 1082W, so overall efficiency obtained is 90%. Simulation is also run for long time to check battery charging time. In constant current mode it took 78 minutes to charge from 30% SoC to 80% SoC. Constant voltage mode applied when battery SoC becomes 80%. In constant voltage mode battery current decreases fast, so it takes long time in hours to charge remaining 20% SoC.

Simulation results Performance parameters:

Power	Vac	PF	THD (%)	Efficiency (%)	Ripple ΔVdc_link (%)
7 kW	200	0.99	2.93	92.71	3.6
	230	0.99	3.36	95.71	3.5
	250	0.99	3.67	96.91	3.3
6 kW	200	0.99	2.93	91.1	3.4
	230	0.99	3.37	93.92	3.4
	250	0.99	3.69	94.1	3.3
5 kW	200	0.99	2.93	90.16	3.2
	230	0.99	3.36	91.88	3.2
	250	0.99	3.67	92.86	3.1
4 kW	200	0.99	2.93	90.6	3.2
	230	0.99	3.37	90.18	3.1
	250	0.99	3.69	90.97	3
3 kW	200	0.99	2.98	90.04	3
	230	0.99	3.38	90.01	3
	250	0.99	3.68	89.65	2.7
2 kW	200	0.99	2.97	86.43	3.1
	230	0.99	3.42	87.42	3
	250	0.99	3.73	89.09	2.7
1 kW	200	0.99	3.04	83.51	1
	230	0.99	3.57	86.15	1.1
	250	0.99	3.87	87.4	0.9
0.5 kW	200	0.99	3.55	66.12	0.4
	230	0.99	4.08	67.69	0.4
	250	0.99	4.52	69.75	0.4

V. CONCLUSION:

The battery charger system based on a complete bridge phase shift converter and quazi-Z-source converter is provided in this study along with extensive analysis and simulation results. A Quazi-Z source converter reduces THD to 3.53%, increases power factor nearly to unity, and lowers DC-link voltage ripples in both voltage and current. Phase-shifted PWM signals control the Full Bridge converter, while the PFC stage is controlled by the hysteresis current control approach. To charge a 48V lithium-ion battery, it reduces the high input DC voltage (400V). An algorithm for constant voltage and constant current control is used with PSFB converters. 90% efficiency was shown by the system, which is intended to produce 1kW of output power.

The suggested system's charging time was found to be 78 minutes, but this can be lowered even more by raising the charger's power rating. The project's future scope will encompass system testing and the actual implementation of hardware. Furthermore, the solar system can be integrated after the rectification stage by utilising the proper switching arrangement at the input side. The input grid AC power is turned off when solar power is available; however, grid supply can be used when solar power is unavailable or during the night.

VI. REFERENCES:

[1] Chia-Chun Tsai, Whei-Min Lin, Chi-Hsiang Lin Ming-Shu Wu, "Designing a Fast Battery Charger for Electric Bikes," 2010 Interational Corerence on System Sience and Engineering, IEEE, Taipei.

[2] Zuzhi Zhang, Haiping Xu, Lei Shi, Dongxu Li, Yuchen Han “Application Research of an Electric Vehicle DC Fast Charger in Smart Grids,” 2012 IEEE 6th International Conference on Information and Automation for Sustainability, 27-29 September 2012, Beijing.

[3] Mohammad Rejwan Uddin, Zaima Tasneem, Saila Ishrat Annie and Khosru M Salim, "A High Capacity Synchronous Buck Converter for Highly Efficient and Lightweight Charger of Electric Easy Bikes," International Conference on Electrical, Computer and Communication Engineering (ECCE), February 16-18, 2017, Cox’s Bazar, Bangladesh.

[4] Shuo Liu, Baoming Ge, Xinjian Jiang, Haitham Abu-Rub, Fang Z. Peng, “A Novel Indirect Quasi-Z-Source Matrix Converter Applied to Induction Motor Drives,” in Energy Conversion Congress and Exposition, IEEE 2013, pp. 2440 - 2444, Denver, CO, USA.

[5] Yam P. Siwakoti, Frede Blaabjerg, Poh Chiang Loh, Graham E. Town, “A High Voltage Gain Quasi Z-Source Isolated DC/DC Converter,” IEEE International Symposium on Circuits and Systems (ISCAS), 01-05 June 2014, Melbourne, VIC, Australia.

[6] Yam P. Siwakoti, Student “Improved Modulation Technique for Voltage Fed Quasi-Z Source DC/DC Converter”, 2014 IEEE Applied Power Electronics Conference and Exposition - APEC 2014, pp. 1973– 1978, Fort Worth, TX, USA.

[7] Yuba Raj Kafle, Saad Ul Hasan, Muhammad Kashif, Jahangir Hossain, Graham E. Town, “A New PWM Shoot-through Control For Voltage-Fed Quasi-Z-Source DC/DC Converter,” IEEE International Telecommunications Energy Conference (INTELEC), 22-26 October 2017, pp. 494 - 497.

[8] Junfeng Liu, Jialei Wu, Jianyong Qiu, And Jun Zeng, “Switched Z-Source/Quasi-Z-Source DC-DC Converters With Reduced Passive Components for Photovoltaic Systems”, IEEE Access, vol. 7, 26 March2019, pp. 40893 – 40903.

[9] Liqiang Yang; Dongyuan Qiu; Bo Zhang; Guidong Zhang; Wenxun Xiao “A quasi-Z-source DC-DC converter,” 2014 IEEE Energy Conversion Congress and Exposition (ECCE), 14-18 September 2014, 10.1109/ECCE.2014.6953500, Pittsburgh, PA, USA.

[10] A. Hadi, I. Said, M. Mansor, H. Hussain, “Fast Charger for Li-ion Batteries Based on Battery Temperature,” 3rd IET International Conference on Clean Energy and Technology (CEAT) 2014, 24-26 November 2014, Kuching.

[11] Oladimeji Ibrahim, Nor Zaihar Yahaya, Nordin Saad, K. Y. Ahmed, “Design and Simulation of Phase-Shifted Full Bridge Converter for Hybrid Energy Systems,” 6th International Conference on Intelligent and Advanced Systems (ICIAS), 15-17 August 2016, Kuala Lumpur, Malaysia.

[12] Juncheng Lu, Kevin Bai, Allan Ray Taylor, Guanliang Liu, Alan Brown, Philip Mike Johnson, Matt McAmmond, “A Modular Designed Three-phase High-efficiency High-power-density EV Battery Charger Using Dual/Triple-Phase-Shift Control,” IEEE Transactions on Power Electronics, vol. 33, no. 9, September 2018, pp. 8091 – 8100.

[13] Yongzhe Sun, Bin Jiao, “Design of a Soft-Switched Phase-Shift Full Bridge Converter”, 2016 3rd International Conference on Systems and Informatics (ICSAI), 09 January 2017, pp. 230-234, Shanghai, China.

[14] Cheng Pu, Zhenyang Hao, Chenmao Shao, Xiaoyong Ren, “Two- stage Interleaving DC/DC Topology Based on Phase-shift Full bridge Converter,” IEEE International Conference on Electrical Systems for Aircraft, Railway, Ship Propulsion and Road Vehicles & International Transportation Electrification Conference (ESARS- ITEC), 07-09 November 2018, Nottingham, UK.

[15] Amol R. Sutar, Suhas H. Mhabadi, Mahadev S. Patil “Design and Implementation of Quasi Z-source Converter Based Battery Charger for Electric Vehicles”, 2023 IEEE 8th International Conference for Convergence in Technology (I2CT), 7-9 April 2023, India